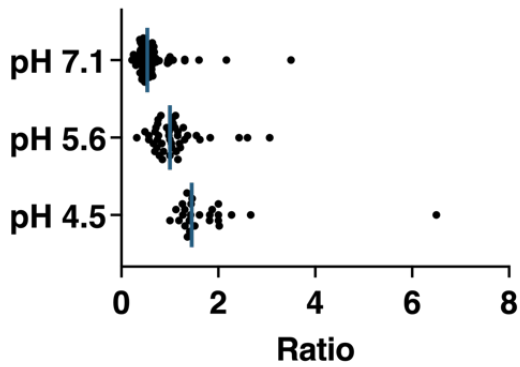


A.



B.

pH	Mean Ratio	SEM	n
4.2	1.73	0.12	32
4.5	1.79	0.20	27
5.0	1.48	0.08	39
5.2	1.17	0.04	45
5.6	1.09	0.08	44
6.0	0.88	0.06	37
6.2	0.66	0.04	48
7.1	0.63	0.05	86
7.4	0.74	0.05	84

Figure S1. **The pH sensitivity of the mTFP1-mCitrine FRET pair.** A. Fluorescence intensity ratio data for individual virus particles from the experiment in Figure 1C is plotted at three pH values where each dot represents the emissions intensity ratio (494-502nm)/(530-538nm) for one particle. Blue bars represent the median ratio value of all particles at that pH. B. The fluorescence intensity ratio values (494nm/530nm) from the plot in Figure 1C. The number of individual particles at each pH varied in part because particles lifted from the coverslip or, in some cases, did not fluoresce above background at standard imaging settings at low pH. All data in A and B are from a single preparation of virus.

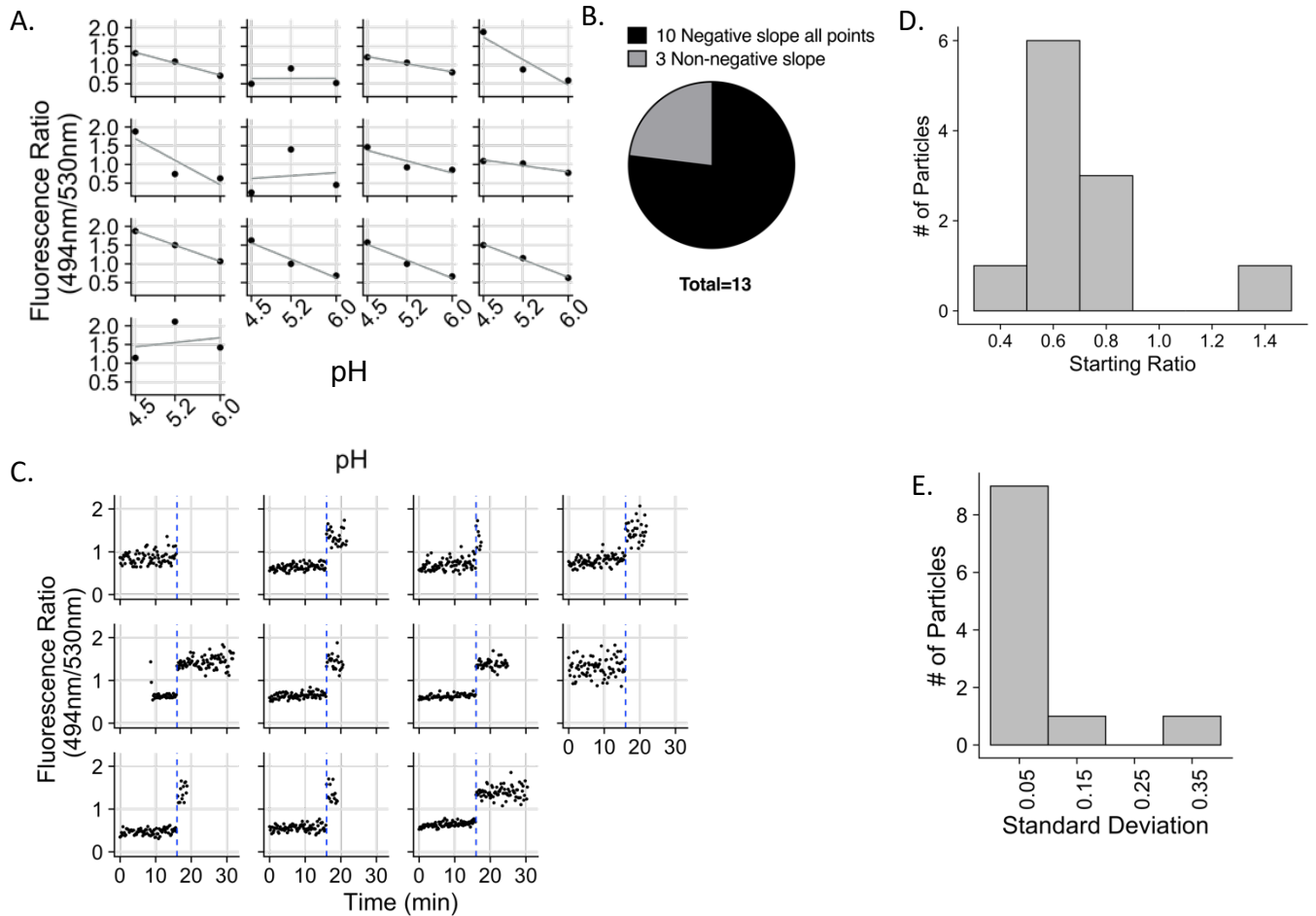
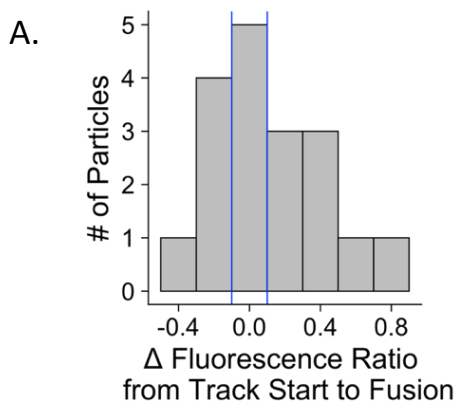


Figure S2. Variability of fluorescence behavior and pH response of viral particles with the mTFP1-mCitrine FRET pH sensor on coverslips. A. Particles spun onto a poly-lysine coverslip were imaged in three buffers of known pH consecutively applied and the 494nm/530nm emission intensity ratio of 13 individual particles was determined. B. Proportion of particles in A that show the expected progression of increasing ratio with decreasing pH for all points (negative slope) versus proportion of particles that do not show this expected behavior (non-negative slope). C. Particles spun onto a poly-lysine coverslip were imaged in pH 7.1 buffer every 12s. After 16 min, pH 5.2 buffer was added as represented by the vertical dashed line. 494nm/530nm fluorescence intensity ratios are graphed over time. D. Distribution of the emission intensity ratio (494nm/530nm) of the experiment in panel A averaged over the first 6 frames. E. Distribution of standard deviations of the 494nm/530nm fluorescence intensity ratios over the first 6 frames of each experiment in panel C, representing frame-to-frame variability for individual particles.



B.

Time (minutes)	Fluorescence Ratio (494nm/530nm)	pH	Δ pH per minute	Δ pH per minute, to and from local minimum
36.3	0.99	5.7		
38.0	1.14	5.4	-0.14	
40.0	1.81	less than 4.2	At Least -0.61	At least -0.40
41.3	1.52	4.8	0.49	
42.3	1.05	5.6	0.72	At Least 0.59

C.

Time (minutes)	Fluorescence Ratio (494nm/530nm)	pH	Δ pH per minute	Δ pH per minute, to and from local minimum
33.0	1.0	5.6		
36.0	1.6	4.7	-0.30	
36.7	2.0	Less than 4.2	At least -0.75	At least -0.38
39.0	1.1	5.5	0.56	At least 0.56

Figure S3. Additional acidification characteristics of endosomes harboring viral particles that fuse. A. Frequency histogram of the difference of 494nm/530nm emission intensity ratios between the mean of the six frames over which the particles are first observed (start) and the time at which the particles fuse (fusion). Blue lines denote the “zero” bin that contains particles within the band of frame-to-frame variability of the FRET sensor, i.e. particles displaying insignificant ratio changes. B. Quantification of a rapid fluctuation in pH in a fusion permissive endosome beginning about 5 minutes following fusion of the viral particle. The fluorescence ratio over the entire observation time is depicted in Fig. 3A panel i. C. Quantification of a pH fluctuation in an endosome occurring in a time window 5-10 minutes prior to the fusion of the viral particle. The fluorescence ratio over the entire observation time is depicted in Fig. 3A panel xvii. For B and C, when fluorescence ratio values fell above the upper limit of the calibration curve, the pH was less than 4.2 but the exact value of the pH could not be determined. The values listed in the right are for the rate of pH change per minute over the entire time segment leading to the highest ratio (lowest pH value) and over the time period of re-alkalization to baseline.

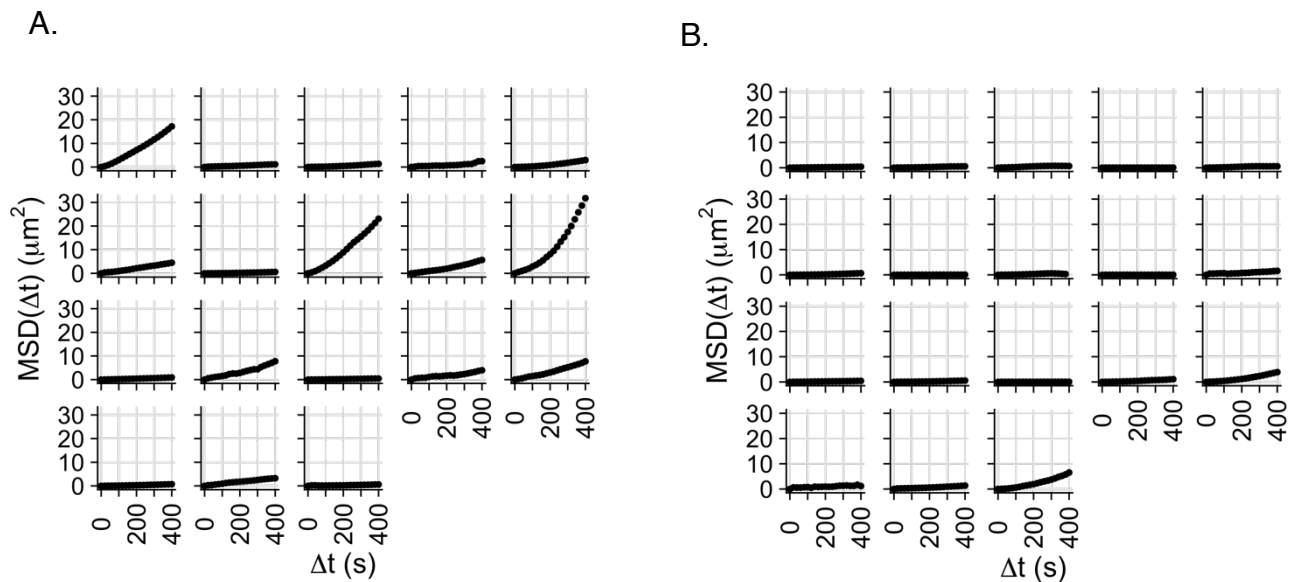


Figure S4. **Motion analysis for individual endosomes harboring fusing and non-fusing viral particles.** A. The mean squared displacement (μm^2) was calculated from particle localizations generated from tracking and plotted up to a maximum time step of 400 seconds for all fusion-permissive endosomes. The smallest time step is 20 seconds. B. Same as A., for fusion non-permissive endosomes. The averaged data from panels A. and B. are presented in Figure 6A.

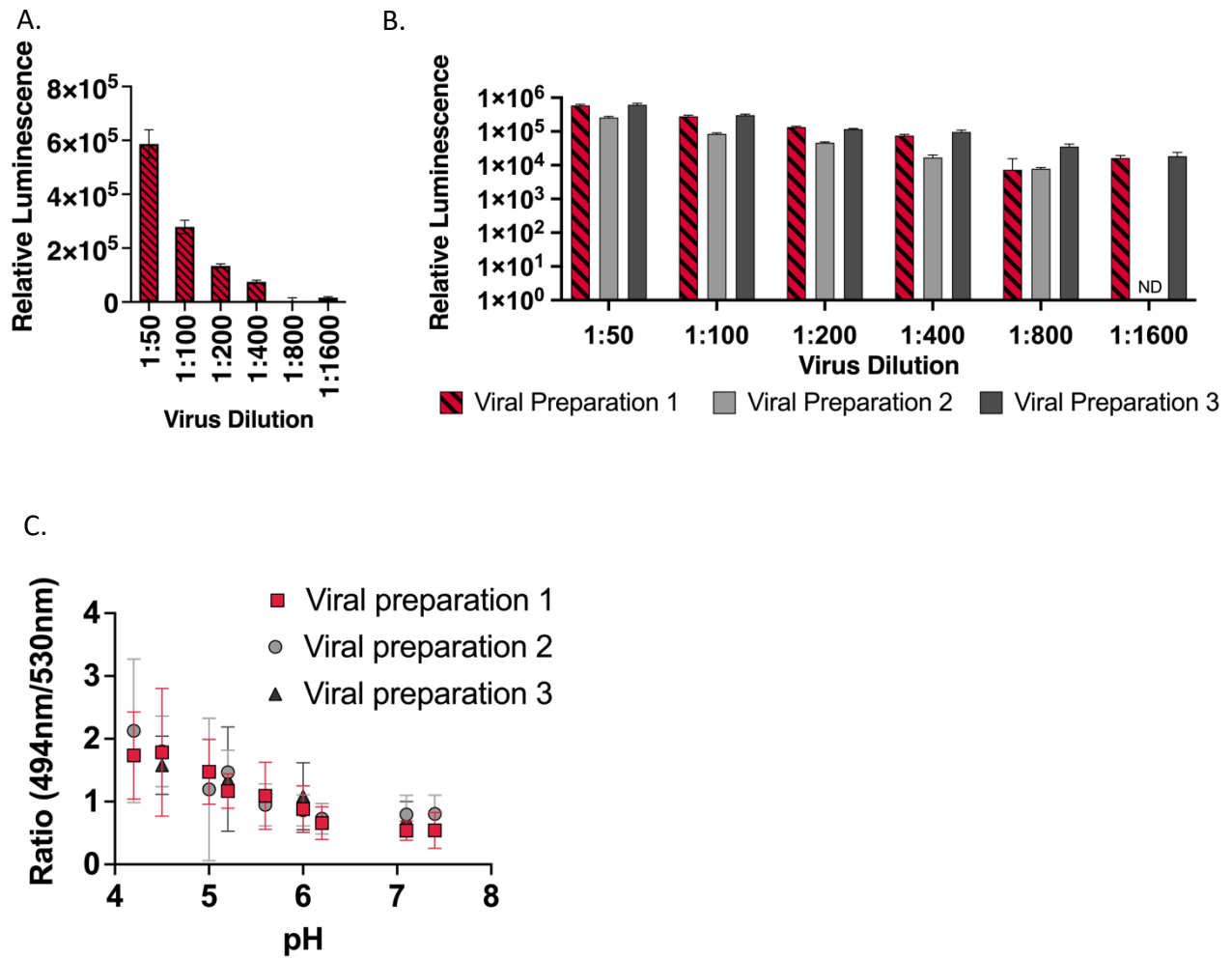


Figure S5. Infectivity and calibration curves of viral particles pseudotyped with VSV-G, bearing the pH sensor mTFP1-mCitrine and the content marker Gag-mKate2. A) The infectivity of pseudovirus used in imaging experiments from which the data displayed in Figures 1-6 originates. B) Infectivity data as in panel A (shown as red striped bars) alongside infectivity data for two other viral preparations produced using the same procedure as for the preparation in panel A. For viral preparation 2, the 1:1600 dilution was not assessed (indicated by ND). **Data in (B) is plotted on a log scale.** (A-B) Cells were infected as described in the Materials and Methods and the level of infection was measured by luciferase assay. **Relative luminescence units, where a higher value indicates a greater degree of infection, are plotted for several viral dilutions.** Data represent average luminescence units \pm 1SD, measured in triplicate, from one experiment. C) Calibration curves of the pH-sensitive FRET pair for the three viral preparations whose infectivities are shown in panel B. The calibration values are depicted as red squares for the viral preparation whose infectivity is shown in panels A and B (Viral Preparation 1) and whose calibration is also shown in Fig. 1C. For viral preparation 3, data was collected at pH 4.5, 5.2, 6.0 and 7.1 only. Error bars represent 1 SD of the fluorescence ratios of individual particles found in each pH condition. For each pH condition, at least 32 individual particles were measured.